A Sampling Theorem for Exact Identification of Continuous-time Nonlinear Dynamical Systems

Zhexuan Zeng, Zuogong Yue, Alexandre Mauroy, Jorge Gonçalves and Ye Yuan

I. Numerical experiments

Several dynamical systems are identified from time-series with different sampling periods. The critical sampling period and identification errors with growing sampling periods are compared to verify the sampling criterion. Koopman-based approach [1] is used for identification since it does not need to calculate the derivatives of states and can identify dynamical systems using measurements with lower sampling frequency.

We consider the vector field

$$f_k(\boldsymbol{x}) = \sum_{j=1}^{N} w_j^k g_j(\boldsymbol{x}),\ k = 1, \ldots, n,$$

where $g_j(\boldsymbol{x})$ are monomial basis functions and coefficients w_j^k are to be identified. Consider the finite-dimensional observable space $\mathcal{F}_m = \mathrm{span}\{g_1, g_2, \ldots, g_N\}$, where $g_j(\boldsymbol{x}) \in \{\boldsymbol{x}_1^{s_1} \ldots \boldsymbol{x}_n^{s_n} | (s_1, \ldots, s_n) \in \mathbb{N}^n, s_1 + \ldots + s_n \leq m\}$ and $\boldsymbol{x}_j (1 \leq j \leq n)$ is the jth component of $\boldsymbol{x}$. Assume that the dynamical system can be approximated by a linear system in this this observable space $\mathcal{F}_m$. By lifting the data to $\mathcal{F}_m$, the matrix of linear Koopman operator $\widehat{U}$ and generator $\widehat{L}$ can be obtained. The coefficients of the vector field can be recovered as $\hat{w}_j^k = [\widehat{L}]_{jl}$ with basis functions $g_l(\boldsymbol{x}) = \boldsymbol{x}_k$. The normalized root-mean-square error (NRMSE) of coefficients is computed to describe the identification error of the vector field:

$$\mathrm{RMSE} = \sqrt{\frac{1}{nN} \sum_{k=1}^{n} \sum_{j=1}^{N} (\hat{w}_j^k - w_j^k)^2},$$

$$\mathrm{NRMSE} = \mathrm{RMSE}/|w|,$$

where $|w|$ is the average value of all nonzero coefficients w_j^k of associated dynamical systems, i.e.,

$$|w| = \sum_{k=1}^{n} \sum_{j=1}^{N} |w_j^k|/q,$$

where q is the number of non-zero coeffficients. The dynamical systems for identification are as follows:

Zhexuan Zeng, Zuogong Yue and Ye Yuan are with School of Artificial Intelligence and Automation, Huazhong University of Science and Technology, Wuhan, China.

A. Mauroy is with the Department of Mathematics and the Namur Institute for Complex Systems (naXys), University of Namur, 5000 Namur, Belgiumand.

J. Gonçalves is with the Luxembourg Centre for Systems Biomedicine, University of Luxembourg, 4367 Belvaux, Luxembourg.

*Email: yye@hust.edu.cn

a) Linear system with states $\boldsymbol{x} = [x_1, x_2]^T$.

$$\begin{aligned} \dot{x}_1 &= 0.1x_1 + 3x_2, \\ \dot{x}_2 &= -3x_1 + 0.1x_2. \end{aligned} \tag{1}$$

In the Koopman-based identification approach, we set 1000 trajectories, 30 snapshots at times for each trajectory and the random initial condition $\boldsymbol{x}(t_0) \in [-1, 1]^2$. In order to minimize the impact of other factors such as the choice of observable space on error of identification, we select the smallest Koopman invariant space, i.e., $m = 1$.

The critical sampling period is analyzed as follows. For the linear system (1), the eigenspace $\mathcal{F}_2$ is the space of state observable functions $\mathrm{span}\{g_1(\boldsymbol{x}) = x_1, g(\boldsymbol{x}) = x_2\}$. In this space, the generator associated with the system (1) can be represented by the following system matrix with the basis functions g_1, g_2:

$$L|_{\mathcal{F}_2} = \begin{pmatrix} 0.1 & 3 \\ -3 & 0.1 \end{pmatrix}$$

Thus the eigenvalues are determined by

$$(\lambda - 0.1)^2 + 3^2 = 0,$$

leading to

$$\lambda_{1,2} = 0.1 \pm 3i.$$

The theoretical lower bound of sampling frequency is $2 \max |\mathrm{Im}(\lambda(L|_{\mathcal{F}_2}))| = 6$ rad/s and the critical sampling period is $\pi / \max |\mathrm{Im}(\lambda(L|_{\mathcal{F}_2}))| = \pi/3$ s. The lower bound of sampling frequency will be integer multiples of 6 rad/s if other Koopman valid eigenspace $\mathcal{F}_2$, spanned by multiplications of these eigenfunctions, are used to analyze the lower bound.

Fig. 1(a) shows the comparison of critical sampling period and NRMSE of the linear dynamical system. The blue line shows the result of NRMSE with growing sampling periods. The red dashed line denotes the critical sampling period $\pi/3$. It is in agreement the theorem that the NRMSE changes significantly as T_s tends to the red line.

b) Nonlinear systems with a fixed point at $[0, 0]$:

$$\begin{aligned} \dot{x}_1 &= -3x_2 - x_1(x_1^2 + x_2^2), \\ \dot{x}_2 &= 3x_1 - x_2(x_1^2 + x_2^2). \end{aligned} \tag{2}$$

We set 1000 trajectories, 30 snapshots at times for each trajectory and random initial condition $\boldsymbol{x}(t_0) \in [-1, 1]^2$ for identification. In order to make the comparison of sampling period bound and the change of NRMSE with growing sampling period more convincing, three eigenspaces $\mathcal{F}_m, m =$

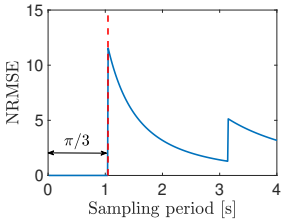

(a) Identification error

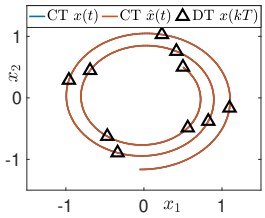

(b) State prediction ($T = 0.5$ s)

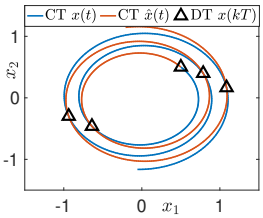

(c) State prediction ($T = 1.1$ s)

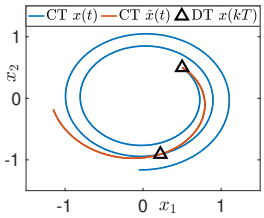

(d) State prediction ($T = 2.8$ s)

Fig. 1. Identification errors with growing sampling periods (a) and prediction by vector field identified from data with sampling period $T = 0.5$ s (b), $T = 1.1$ s (c) and $T = 2.8$ s (d) of linear system. The parameter of observable space is $m = 1$ for prediction.

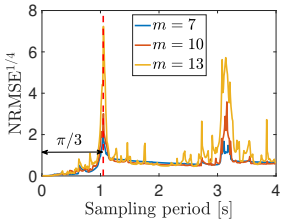

(a) Identification error

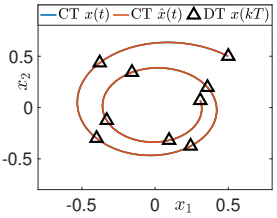

(b) State prediction ($T = 0.5$ s)

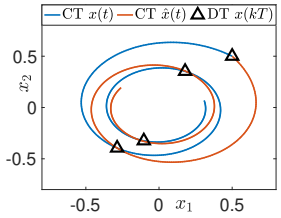

(c) State prediction ($T = 1.1$ s)

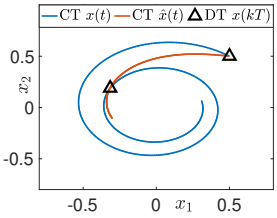

(d) State prediction ($T = 2.8$ s)

Fig. 2. Identification errors with growing sampling periods (a) and prediction by vector field identified from data with sampling period $T = 0.5$ s (b), $T = 1.1$ s (c) and $T = 2.8$ s (d) of nonlinear system with fixed point (2). The parameter of observable space is $m = 13$ for prediction.

$7, 10, 13$ are chosen to approximate the Koopman invariant space for the nonlinear system (2).

For nonlinear systems with fixed point x^*, i.e., $f(x^*) = 0$, the so-called principal Koopman eigenvalues λ_i are the eigenvalues of the Jacobian matrix of the vector field f at the fixed point x^* [2]. Therefore, eigenvalues of the generator of the system (2) are eigenvalues of the Jacobian matrix at origin:

$$J = \begin{pmatrix} 0 & -3 \\ 3 & 0 \end{pmatrix}$$

It leads to the principal Koopman eigenvalues being $\pm 3i$. The lower bound of sampling frequency is 6 rad/s and the critical sampling period is $\pi/3$ s. Other Koopman eigenvalues can be obtained by taking linear combinations (with weights that are positive and integers) of these principal eigenvalues. The bound of sampling frequency analyzed by associated eigenfunctions will be integer multiples of 6 rad/s.

The critical sampling period $\pi/3$ is denoted as the red dashed line in Fig. 2(a). It shows that the NRMSE$^{1/4}$ of the nonlinear system (2) appears to peak when the sampling period grows close to the red dashed line in every observable space we choose, which is in agreement with the critical sampling period.

Consider a nonlinear system with a stable limit cycle at $r = \sqrt{x_1^2 + x_2^2} = 1$:

$$\begin{aligned} \dot{x_1} &= 3x_2 - x_1(x_1^2 + x_2^2 - 1), \\ \dot{x_2} &= -3x_1 - x_2(x_1^2 + x_2^2 - 1). \end{aligned} \tag{3}$$

We set 1000 trajectories, 30 snapshots at times for each trajectory and random initial condition $\boldsymbol{x}(t_0) \in [-1.5, 1.5]^2$ to identify this system. Moreover, three eigenspaces $\mathcal{F}_m, m = 7, 10, 13$ are used to approximate the Koopman invariant space for the nonlinear system (3).

The principal Koopman eigenvalues are calculated as follows. Using polar coordinates, i.e., $x_1 = r\cos\theta$ and $x_2 = r\sin\theta$, we obtain the dynamical system

$$\begin{aligned} \dot{r} &= -r^3 + r, \\ \dot{\theta} &= -3. \end{aligned}$$

For dynamical systems that admit limit cycles, the Floquet exponents are principal Koopman eigenvalues [2]. Since the limit cycle is at $r = 1$, the eigenvalue (Floquet exponent) is -2. Other principal eigenvalues are $\pm 3i$ with associated eigenfunction $e^{\pm i\theta}$. The critical sampling period is $\pi/3$ s.

Fig. 3(a) shows the NRMSE$^{1/4}$ for the identification and the critical sampling period $\pi/3$ s. The NRMSE$^{1/4}$ changes significantly as sampling periods tend to ($m = 7, 10$) or a little earlier ($m = 13$) than $\pi/3$, which is consistent with the critical sampling period. This numerical example also suggests that it may not always be better to use a large number of observable functions.

It can be seen that the NRMSE drops for a while then rises again since the sampling frequency exceeds the critical sampling period. To study this phenomenon, the states generated by the identified dynamical system $\hat{\boldsymbol{x}}(t)$ and the real states $\boldsymbol{x}(t)$ are visualized in Fig. 1(b)-Fig. 1(d), Fig. 2(b)-Fig. 2(d), Fig. 3(b)-Fig. 3(d) when the sampling period are 0.5s, 1.1s and 2.8s. These typical sampling periods show the results of identified vector fields when associated sampled data "capture", "suddenly miss" and "wrongly approach" the correct dynamical system, respectively. The blue lines denote the true states of time $\boldsymbol{x}(t)$ with the initial condition $[0.5, 0.5]$. The orange lines are the prediction of states $\hat{\boldsymbol{x}}(t)$ by identified vector fields $\hat{f}$. It can be inferred that the directions of vector fields seem like rotating with the increasing of sampling period to find the most simple trajectory matching the measurements. Fig. 3(b) shows the predictions

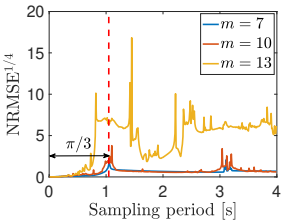

(a) Identification error

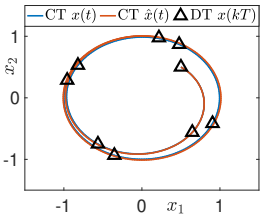

(b) State prediction ($T = 0.5$ s)

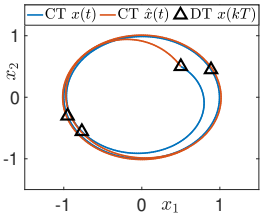

(c) State prediction ($T = 1.1$ s)

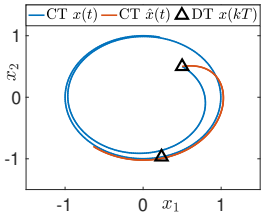

(d) State prediction ($T = 2.8$ s)

Fig. 3. Identification errors with growing sampling periods (a) and prediction by vector field identified from data with sampling period $T = 0.5$ s (b), $T = 1.1$ s (c) and $T = 2.8$ s (d) of nonlinear system with limit cycle (3). The parameter of observable space is $m = 13$ for prediction.

that sampled data are able to capture the correct systems. When the sampling period exceeds the critical sampling period, the direction of identified vector field $\hat{f}$ at each $\boldsymbol{x}$ is almost opposite to the truth and the NRMSE curve has a peak (see for example the prediction when the sampling period is 1.1s in Fig. 3(a)). After that, the direction of $\hat{f}$ at each $\boldsymbol{x}$ continues rotating. Therefore, the difference between $\hat{f}$ and the truth decreases as illustrated in Fig. 3(d).

REFERENCES

[1] A. Mauroy and J. Gonçalves, "Koopman-based lifting techniques for nonlinear systems identification," *IEEE Transactions on Automatic Control*, vol. 65, no. 6, pp. 2550–2565, 2019.

[2] A. Mauroy and I. Mezić, "Global stability analysis using the eigenfunctions of the koopman operator," *IEEE Transactions on Automatic Control*, vol. 61, no. 11, pp. 3356–3369, 2016.